Chalcogenide Letters Vol. 22, No. 10, October 2025, p. 871 - 882

Performance evaluation of CdTe-based heterojunction solar cell with IGZO-based window layer and electron transport layer

R. K. Mishra [a *], M. N. Anwar [a], M. A. Hasan [b]
[a] *Department of Electrical Engineering, National Institute of Technology Patna, Bihar, 800005 India*
[b] *Department of Electrical and Electronics Engineering, Birla Institute of Technology Mesra, Ranchi, 835215 India*

This study introduces a novel approach to enhancing the performance of CdTe/IGZO-based heterojunction solar cells by utilizing IGZO as both a window layer and an electron transport layer (ETL). A comprehensive simulation using SCAPS-1D was conducted to evaluate the impact of various transparent conductive oxides (TCOs), including ITO, SnO_2, ZnO, and FTO, on key photovoltaic parameters such as power conversion efficiency (PCE), open-circuit voltage (Voc), short-circuit current density (Jsc), and fill factor (FF). The research also explores the critical role of transport layers (HTL/ETL) and their material properties, band alignment, carrier mobility, and defect density, in optimizing device performance. The study's key contribution lies in identifying ITO as the most effective TCO due to its superior electron mobility, while highlighting the trade-offs associated with SnO_2 and ZnO, which exhibit enhanced optical properties but comparatively moderate performance. Furthermore, FTO is shown to yield the poorest results, underscoring the significance of TCO selection in thin-film solar cell design. By offering a detailed comparative analysis and optimization insights, this work provides a strategic pathway for developing high-efficiency, cost-effective CdTe/IGZO-based solar cells, advancing next-generation thin-film photovoltaic technologies.

(Received July 4, 2025; Accepted October 6, 2025)

Keywords: Solar cells, Transparent conductive oxides (TCOs), SCAPS 1D, PCE, ETL, HTL

1. Introduction

Rapid population growth and heavy industrialization have significantly heightened global energy demand. Despite advances, a substantial portion of this demand is still reliant on non-renewable fossil fuels. The fossil fuels, after burning, release carbon dioxide (CO_2) into the atmosphere, thereby not only polluting the environment but also intensifying the greenhouse effect. But due to their depleting resources, researchers are compelled to explore alternative energy sources such as wind, solar, and fuel cells. These sources not only alleviate the bad effects of burning fossil fuels on the environment but also provide a low operational cost[1,2].

Out of the various renewable sources of energy available the solar energy has emerged as one of the leading energy sources because of its availability in abundance as well as ease of implementation. Though a lot of technological advancements have been made in the past year to harness electrical energy from the solar cell still its power conversion efficiency (PCE) is still quite low. This poses a greater challenge to the researchers because the current efficiencies still fall below the theoretical Shockley–Queisser (SQ) limit, which is approximately 35% [3,4].

The structure of the photovoltaic solar cell is classified as a superstrate and substrate configuration. The classification is based on the direction of light penetration into the structure. In the case of a superstrate structure, photons of light pass through the glass substrate, which is typically called transparent conductive oxide (TCO), that acts like a window layer to reach the solar cell. The rest of the photovoltaic solar cell consists of an absorber layer, and in the more advanced configurations, a sequence of Electron Transport Layer (ETL), buffer layer, absorber layer, and Hole Transport Layer (HTL) [5].

Corresponding author: rajm.phd20.ee@nitp.ac.in
https://doi.org/10.15251/CL.2025.2210.871

Silicon is the main element of the photovoltaic solar cell and has dominated the photovoltaic market for a long time, owing to its reliable performance. But because of the involvement of the high manufacturing cost, its broad adoption has been hampered, urging researchers to explore alternative materials. Particularly, the focus has been shifted towards compound semiconductors, like group II-VI materials, due to their intrinsic photovoltaic properties. In this context, one of the cost-effective heterojunction structures is cadmium telluride (CdTe)-based solar cells, which are often paired with cadmium sulfide (CdS). This combination offers the added advantage of low fabrication cost, approximately 40% lower than silicon-based technologies and 30% lower than copper indium gallium selenide (CIGS) solar cells [6,7].

CdTe is a p-type polycrystalline material having a direct band gap of 1.5 eV and an excellent absorption coefficient (10^5/cm), which makes it an outstanding absorber layer due to its optimal band alignment. The high absorption coefficient of CdTe makes it a highly efficient solar cell due to its ability to absorb nearly 99% of incident photons with minimal thickness [8]. For the window layer, n-type CdS is widely employed due to its favorable band gap of 2.4 eV, which works excellently in the visible range of the light. This combination provides a robust heterojunction along with an efficient solar cell. Recent technological advancements have improved the laboratory-scale efficiency of CdTe/CdS solar cells to 22.1% as of 2022 [9].

To achieve higher efficiencies in CdTe solar cells, researchers have investigated alternative buffer materials to replace CdS. Numerical simulations indicate that using 3C-SiC as the buffer can yield efficiencies of around 17–18% [1]. Zn-based chalcogenides such as ZnO, ZnSe, and ZnS have also been explored, with reported efficiencies reaching up to 23–24%, surpassing those obtained with CdS [2]. In contrast, experimental studies on Mg-doped ZnO (MZO) buffers have demonstrated device efficiencies of approximately 16.1%[3].

To further improve the PCE of the solar photovoltaic cell, hole transport layer (HTL), such as NiO, MoO_x, WO_3, and V_2O_5 are commonly used, whose role is to extract the holes efficiently by reducing the energy barrier at the interface surface. The reduced energy barrier minimizes recombination losses and enhances charge transport. Out of the mentioned HTLs, NiO stands out for its high work function (5 eV) and wide band gap (3.5–3.8 eV), facilitating efficient hole transport and ohmic contact formation [13].

ETL(electron transport layer) plays a crucial role in enhancing solar cells by efficiently extracting and transporting electrons from the absorber layer to the electrode while minimizing recombination losses. Materials like TiO_2,Zno and SnO_2 have demonstrated excellent performance as ETL candidates, contributing to improved stability and efficiency under varying environmental conditions [14]. Transparent conductive oxide (TCO) material is the topmost layer of the superstrate structure, thereby providing not only mechanical support but also electrical conductivity. Common TCO materials include Indium Tin Oxide (ITO) and Fluorine-doped Tin Oxide (FTO), both known for their high transparency in the visible spectrum. Alternative materials such as TiO_2, SnO_2, and ZnO have also been explored, expanding the range of options for solar cell applications [15].

Although the combination of CdTe/CdS photo voltaic solar cells provides a good PCE value, but is still less than the theoretical Shockley–Queisser (SQ) limit. This study contributes to this ongoing effort by focusing on the numerical optimization of solar cells using CdTe as the absorber layer and Indium Gallium Zinc Oxide (IGZO) as a multifunctional material. With its direct band gap of 3.6 eV, IGZO effectively minimizes absorption losses, enhancing the overall efficiency of the solar cell. Simulations performed using SCAPS-1D software aim to provide new insights into the role of IGZO and other material configurations in achieving higher photovoltaic performance [16].

This paper builds on the insights gained from the existing literature on CdTe/CdS solar cells, focusing on numerical optimization to further enhance their performance. While previous studies have explored alternative buffer materials and their influence on power conversion efficiency (PCE), this work investigates the potential of Indium Gallium Zinc Oxide (IGZO) as an innovative material in the solar cell structure. Using SCAPS-1D simulation software, the impact of IGZO's direct band gap and optical properties on minimizing absorption losses and improving PCE is thoroughly analyzed. The findings from this study not only contribute to addressing the limitations of conventional CdS buffer layers but also demonstrate the role of IGZO in achieving higher efficiencies under varying operational conditions.

The proposed work presents a novel approach to design solar cell so that an increased efficiency has been achieved. The paper has been drafted as follows. Section 1 presents the introduction and literature review related to the state of the art in the domain. Section 2 briefly presents a review of existing solar cell structures and presents the proposed solar cell structure. The associated mathematical model to analyze the performance of the solar cell has been presented in section 3. Section 4 presents the simulation analysis and results to establish the novelty of the proposed design and the claim of enhanced efficiency. The conclusion follows next.

2. Numerical modeling and device structure

Numerical modelling is a cornerstone of solar cell research, enabling the analysis and optimization of device performance by simulating various material properties, device architectures, and environmental conditions. Several simulation tools, such as AMPS-1D, SILVACO ATLAS, wxAMPS, COMSOL, and SCAPS-1D, are widely employed for this purpose. These tools provide researchers with the capability to model and evaluate critical parameters such as open-circuit voltage (VOC), short-circuit current density (JSC), fill factor (FF), power conversion efficiency (PCE), and temperature-dependent performance. They also allow for an in-depth analysis of recombination mechanisms, carrier transport, and device stability, all of which are essential for designing efficient solar cells.

Among these tools, SCAPS-1D offers unique features that make it particularly suitable for thin-film solar cell research. It supports up to seven-layer device structures and includes a database of buffer layer materials commonly used in heterojunction devices. SCAPS-1D allows for the simulation of electrical and optical characteristics, including current-voltage curves under illuminated and dark conditions, as well as temperature-dependent analyses. These capabilities enable researchers to study recombination profiles and carrier distribution, which are critical for understanding and optimizing device performance.

While each simulation tool has its strengths, the choice of SCAPS-1D in this study is based on its balance between user accessibility and technical versatility. Its ability to simulate multilayer structures and its focus on thin-film solar cells align with the requirements of the device structure under investigation. By leveraging SCAPS-1D, this work aims to provide insights into the influence of material properties and layer configurations on the performance of solar cells, thereby bridging the gap between numerical modelling and experimental validation[17].

2.1. Proposed solar cell structure

The development of high-performance solar cells relies heavily on optimizing the selection and arrangement of material layers to achieve improved efficiency, stability, and environmental compatibility. Each layer in a solar cell plays a crucial role, from light absorption and charge carrier separation to transport and collection. Traditional materials like CdS and other similar compounds, though widely used as buffer layers in CdTe-based solar cells, present inherent limitations, including lower optical transparency, reduced carrier mobility, and environmental concerns due to cadmium toxicity. These challenges have spurred research into alternative materials and innovative layer configurations to address these drawbacks while maximizing solar cell performance. The introduction of advanced materials such as Indium Gallium Zinc Oxide (IGZO) and NiO offers a pathway to overcome these limitations, enabling superior transparency, enhanced stability, and eco-friendliness. This section explores various solar cell structures, analyzing the impact of different Transparent Conductive Oxides (TCOs), buffer layers, and hole transport layers on the performance of CdTe-based solar cells.

Materials like CdS, ZnS, ZnO, and ZnSe have traditionally been employed in CdTe solar cells, but they exhibit limitations in terms of optical properties, carrier mobility, stability, and environmental impact. These materials tend to absorb more light in the blue spectrum, which can hinder overall device efficiency. Additionally, they often suffer from lower carrier mobility and stability issues, particularly in the case of CdS, which is further burdened by the environmental and health concerns associated with cadmium toxicity.

In contrast, Indium Gallium Zinc Oxide (IGZO) presents several advantages over conventional materials. With a higher bandgap of 3.5–4.0 eV (compared to 2.4 eV for CdS), IGZO offers superior transparency, reduced recombination losses, better carrier mobility, and enhanced stability. Moreover, IGZO is less toxic and more environmentally friendly, addressing critical concerns related to material sustainability. Although the use of indium and gallium makes IGZO relatively expensive, ongoing advancements in processing techniques have the potential to lower these costs. The substantial performance benefits of IGZO justify its higher initial expense, making it a compelling alternative for advanced solar cell designs.

Figures 1-2 present schematic diagrams and energy band configurations of the proposed solar cell structures, demonstrating various configurations and their corresponding components. Figures 1 (a)-1(f) and 2(a)-2(b) depict solar cells with CdTe as the absorber layer and IGZO as the buffer layer, paired with different Transparent Conductive Oxides (TCOs), including SnO_2, ZnO, ITO, and FTO. Fig 1 (a) presents the layer structure of a solar cell with SnO_2 as configuring material and the energy band diagram of this structure is given in Fig 1(b). Similarly structure with SnO and ITO has been presented in Fig 1(c) and Fig. 1(e). Their respective energy band diagrams are presented in Fig. 1(d) and Fig 1(f). Figure 2(c)-2(d) introduces a modified structure that incorporates NiO as the Hole Transport Layer (HTL) alongside the setup in Figure 2(e)-2(f). Finally, Figure 2(e)-2(f) illustrates a design combining CdTe/CdS with NiO as the HTL and IGZO as the Electron Transport Layer (ETL), showcasing the flexibility and potential performance improvements offered by these configurations.

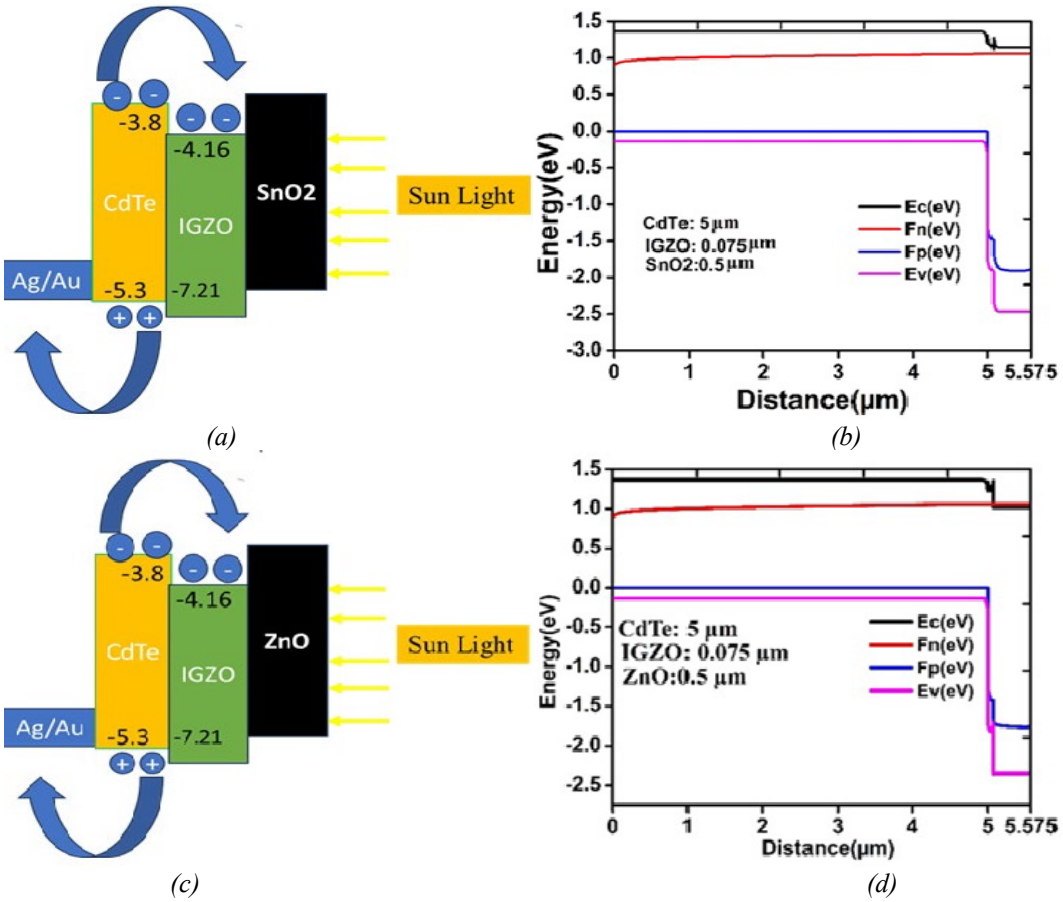

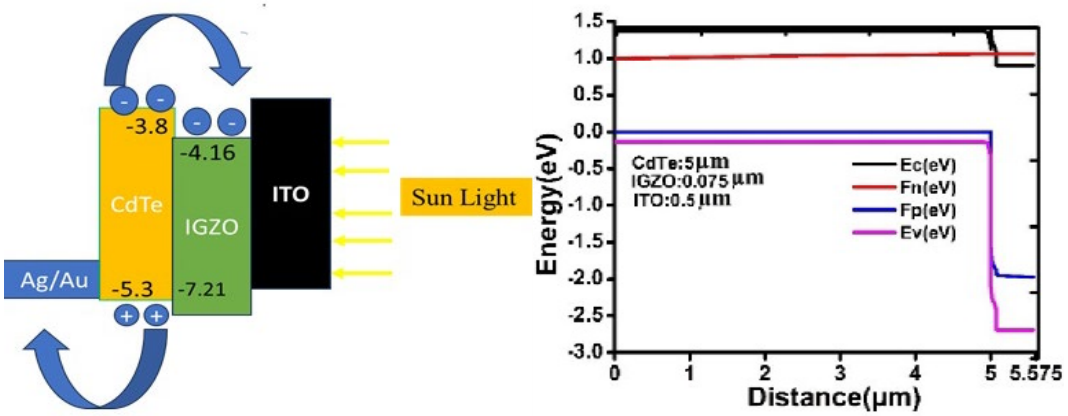

Fig. 1. Different solar PV cell structures with (a) CdTe/IGZ/SnO_2 (b) Energy band diagram (c) CdTe/IGZO/ZnO (d) Energy band diagram (e) CdTe/IGZ/ITO (f) Energy band diagram.

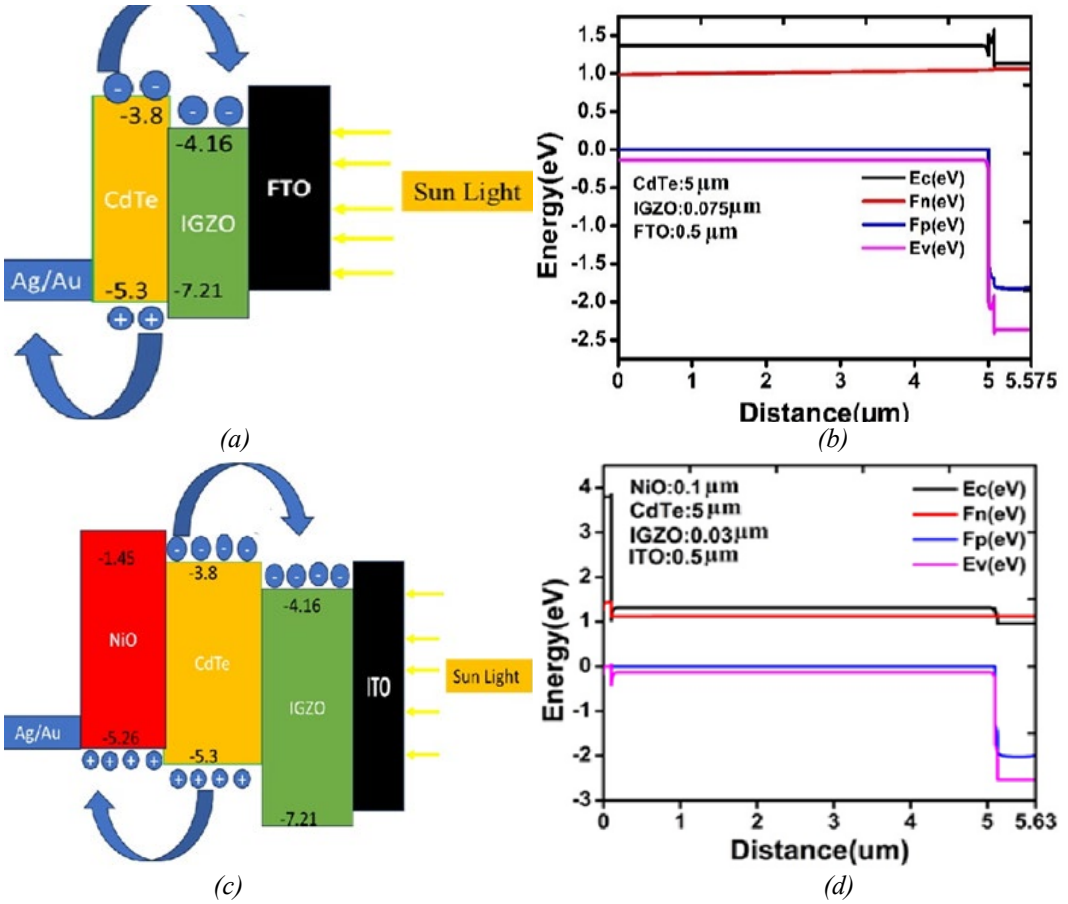

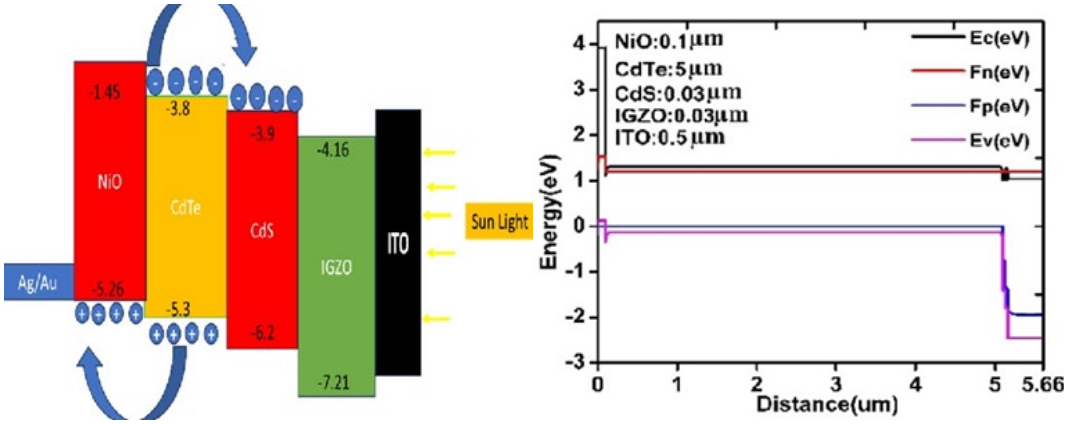

Fig. 2. Solar PV cell structure for (a) CdTe/IGZO/FTO solar cell (b) Energy band diagram (c) CdTe/IGZO/ITO solar cell (d) Energy band diagram (e) NiO/CdTe/CdS/IGZO/ITO solar cell (f) Energy band diagram.

3. Mathematical modeling of the material properties

The numerical modeling of semiconductor devices relies on solving fundamental one-dimensional semiconductor equations to analyze charge carrier dynamics. These equations include Poisson's equation, which governs electrostatic potential distribution, as well as electron and hole continuity equations, which describe carrier transport through drift and diffusion mechanisms. Additionally, recombination and generation processes, along with the effects of electric fields, are considered to evaluate overall device behavior. By solving these equations, numerical models provide insights into key performance parameters such as charge carrier distribution, electric potential, and current-voltage characteristics, aiding in the design and optimization of efficient solar cells. The characteristic equations defining solar cell material properties are given as follows,

$$\frac{\partial}{\partial x}\left(\xi_r \xi_o \frac{\partial N}{\partial x}\right) = -q\left(p - n + N_d^+ - N_A^- + \frac{p_{defect}}{q}\right) \tag{1}$$

$$\frac{\partial}{\partial x}(j_n) = G - U_n - \frac{\partial n}{\partial t} \tag{2}$$

$$\frac{\partial}{\partial x}(j_p) = G - U_p - \frac{\partial p}{\partial t} \tag{3}$$

$$j_n = qn\mu_n E + qD_n \frac{\partial n}{\partial x} \tag{4}$$

$$j_p = qn\mu_p E + qD_p \frac{\partial p}{\partial x} \tag{5}$$

In SCAPS-1D, many technical parameters are used to present the behaviour of charge carriers and their associated behaviour in semiconductor materials. The symbol represents the concentration of holes (positively charged carriers), and denotes the concentration of electrons (negatively charged carriers). The symbols present the densities of ionized donor and acceptor atoms, which show the contribution of free carriers to the semiconductor. The diffusion coefficients for holes and electrons are given as and, respectively, presenting how easily carriers move due to a concentration gradient. Their

mobilities are represented by (for holes) and (for electrons). The generation rate of electron-hole pairs due to light absorption is denoted by G, and the current densities for electrons and holes are shown as and respectively. The elementary charge is represented by q, and the relative and absolute permittivity are given as aid. The symbol indicates the charge density due to defects in the material, which can trap carriers and affect device performance. These parameters are essential for accurately simulating solar cell behaviour using SCAPS-1D[17].

By resolving a series of related differential equations that explain the motion and interaction of charge carriers—electron and hole—within the device, SCAPS-1D models the electrical behavior of solar cells. First, the electrostatic potential across the solar cell structure is calculated by the model. It makes use of a technique that links the local charge distribution to this potential. Free carriers, ionized dopants, and trapped charges from flaws are all included in this. The simulation guarantees that the charge conservation principle governs the movement of both electrons and holes. It balances the recombination processes that result in carrier loss with the generation of charge carriers from light absorption. There are multiple recombination mechanisms in SCAPS. These defects are responsible for Auger recombination, direct electron-hole annihilation (radiative recombination), and Shockley-Read-Hall recombination. Diffusion from concentration gradients and drift from electric fields are used to model carrier movement. The characteristics of the various materials used in the solar cell are also taken into account by the software. It examines interface properties, carrier mobilities, defect densities, and energy band structure. It evaluates the effects of these factors on carrier transport and recombination at each location in the simulation area. The result is a comprehensive, layer-by-layer numerical representation of the solar cell's performance in both light and dark conditions. This enables researchers to assess its functionality and make necessary improvements to the device's design.

4. Simulation and results

This study focuses on the numerical optimization of CdTe-based solar cell configurations by analyzing the effects of key design parameters, including layer thickness variations, temperature fluctuations, and doping density modifications. The impact of these factors on critical performance metrics such as open-circuit voltage (Voc), fill factor (FF), short-circuit current density (Jsc), and power conversion efficiency (PCE) is systematically evaluated. The objective is to enhance the understanding of CdTe-based solar cells and improve their efficiency and stability for practical renewable energy applications.

Numerical simulations have been conducted for various solar cell structures, including CdTe/IGZO/ITO, CdTe/IGZO/FTO,CdTe/IGZO/SnO_2, CdTe/IGZO/ZnO,NiO/CdTe/IGZO/ITO and NiO/CdTe/CdS/IGZO/ITO, using SCAPS-1D software. SCAPS-1D is well-suited for modeling multi-layered solar cells and allows for detailed performance analysis through non-routine measurements. The simulations assess the influence of structural and material parameters on Voc, FF, Jsc, and PCE under different operating conditions. Material properties used in the simulations are derived from both theoretical models and experimental data, ensuring accuracy and reliability in performance predictions. The findings from these simulations contribute to the optimization of CdTe-based solar cell designs, paving the way for more efficient and sustainable photovoltaic technologies. The parameters used for the simulation in this work is given in Table 1.

Table 1. Material parameters for simulation [13],[14],[16],[18],[19].

Parameters	ITO	SnO_2	ZnO	CdTe	CdS	IGZO	FTO	NiO
Thickness(nm)	500	500	500	5000	100	75	500	100
Band Gap,E_g(eV)	3.5	3.6	3.3	1.5	2.4	3.05	3.5	3.8
Electron affinity	4	4	4	4.28	4.5	4.16	4.5	1.46
Dielectric permit	9	10	9	10.3	10	10	10	10.7
Conduction band effective density of states ($1/cm^3$)	2.2×10^{18}	2.2×10^{18}	3.7×10^{18}	9.2×10^{17}	2.2×10^{18}	5×10^{18}	2×10^{18}	2.8×10^{19}
Valence band effective density of states ($1/cm^3$)	1.8×10^{19}	1.8×10^{19}	1.8×10^{19}	5.2×10^{18}	1.9×10^{19}	5×10^{18}	1.8×10^{19}	1×10^{19}
Electron mobility (cm^2/Vs)	20	100	100	320	350	15	100	12
Hole mobility, (cm^2/Vs)	10	25	25	40	25	0.1	20	2.8
Shallow acceptor density ($1/cm^3$)	0	0	0	1×10^{13}-1×10^{17}	0	0	0	1×10^{17}-1×10^{21}
Shallow donor density($1/cm^3$)	1×10^{17}	1×10^{17}	1×10^{18}	0	1×10^{16}-1×10^{21}	1×10^{16} - 1×10^{21}	1×10^{17}	0
Defect density($1/cm^3$)	1×10^{15}	1×10^{15}	1×10^{15}	1×10^{15}	1×10^{15}	1×10^{15}	1×10^{15}	1×10^{15}

4.1. Effect of different TCOs on the prescribed solar cell

This study evaluates the performance of CdTe/IGZO-based solar cells with four different Transparent Conductive Oxides (TCOs) as front contacts: ZnO, SnO_2, ITO, and FTO. In these configurations, CdTe functions as the absorber layer, while IGZO serves as the window layer. A numerical analysis was conducted to assess how different TCOs influence the overall efficiency of the solar cells. The layer thicknesses were fixed at 5 μm for CdTe, 0.075 μm for IGZO, and 0.5 μm for the TCO layer (ZnO, SnO_2, ITO, or FTO). Key performance parameters, including open-circuit voltage (Voc), short-circuit current density (Jsc), fill factor (FF), and power conversion efficiency (PCE or η), were analyzed and are summarized in Table 2. Figure 3 (a) presents the variation of Voc and Jsc for the different configurations, offering insights into efficiency trends.

Table 2. Comparison of Voc, Jsc,FF, and Eta for CdTe/IGZO solar cell with different TCO layers.

Solar cell configuration	**Voc(V)**	**Jsc(mA/cm^2)**	**FF (%)**	**Eta (%)**
CdTe/IGZO/ZnO	1.0408	26.649	85.09	23.6
CdTe/IGZO/SnO2	1.0411	26.9796	84.91	23.85
CdTe/IGZO/ITO	1.0414	26.9899	87.11	24.48
CdTe/IGZO/FTO	1.0438	26.8675	63.53	17.82

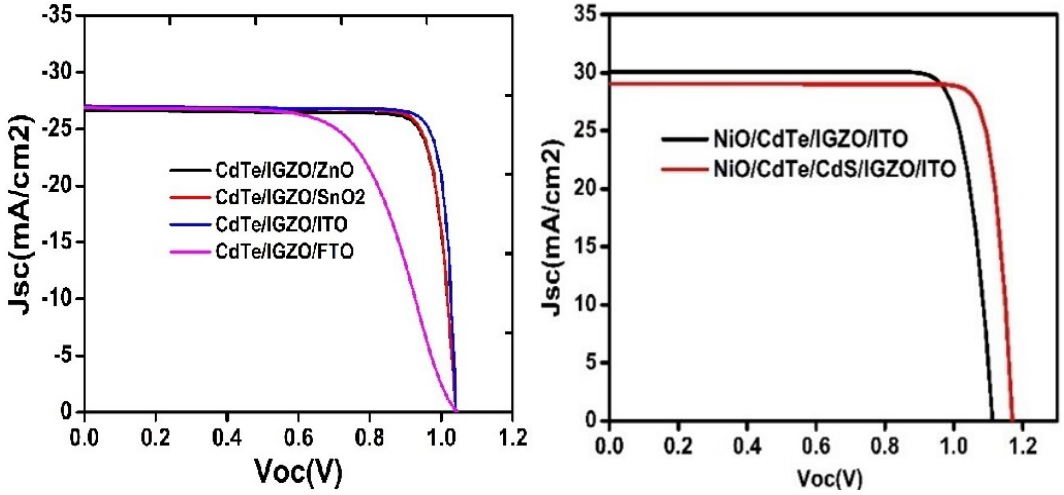

Fig. 3. (a) Comparison between Voc and Jsc for CdTe/IGZo solar cell with different TCOs (b) Voc Vs Jsc graph for NiO/ CdTe/IGZO/ITO and NiO/CdTe/CdS/IGZO/ITO solar cell structures.

The analysis indicates that while Voc, Jsc, FF, and PCE remain nearly constant across all TCO materials, variations in efficiency were observed depending on the choice of TCO. ZnO and SnO_2 exhibited almost identical efficiencies, which aligns with previous studies highlighting their similar electronic properties and conductivity. On the other hand, FTO demonstrated the lowest efficiency among the tested TCOs, likely due to its higher sheet resistance.

Among the tested materials, ITO emerged as the most promising TCO, yielding the highest PCE and overall efficiency. This finding is consistent with earlier studies identifying ITO as an optimal TCO for high-efficiency solar cells, owing to its low resistivity and superior optical transparency. While ZnO and SnO_2 showed comparable performance, concerns regarding their long-term stability and environmental impact must be considered. ZnO, in particular, is prone to degradation under prolonged ultraviolet (UV) exposure, which affects its electrical and optical properties. Additionally, both ZnO and SnO_2 involve production and disposal processes that raise environmental concerns, particularly in terms of pollution associated with their extraction and manufacturing.

Considering efficiency, stability, and environmental impact, ITO stands out as the preferred TCO for CdTe/IGZO-based solar cells. In addition to its superior electrical performance, ITO offers enhanced durability, making it a reliable choice for long-term solar cell applications. Recent studies have further emphasized the importance of stable TCOs in improving solar cell longevity, reinforcing the role of ITO in maintaining efficiency under challenging environmental conditions.

Table 3 presents a comparative analysis of the CdTe/IGZO/ITO solar cell structure with previously reported configurations in which CdTe serves as the active layer. The findings of this study contribute to the ongoing efforts in optimizing TCO selection for high-performance and sustainable solar cell technologies, with ITO proving to be a key material for advancing renewable energy applications.

Table 3. Comparison with different existing structures with CdTe as the active layer.

Solar cell configuration	Voc(V)	Jsc(mA/cm^2)	FF(%)	Eta(%)
CdTe/IGZO/ITO	1.0414	26.9899	87.11	24.48
FTO/MZO/CdTe/Te	0.8	23.4	0.62	11.8
FTO/MZO/CdTe/Au	0.86	25.5	0.73	16.1
FTO/MZO/CdTe/ZnTe:Cu/Au	0.85	28.16	0.81	19.63
AR coating FTO/MZO/CdTe/Te	0.86	26.8	0.79	18.03
ZnO/CdS/CdTe/Au	1.06	24.56	86.46	22.42
CdTe/CdS	0.884	31.73	78.89	22.14
CdTe/ZnSe	0.876	32.09	81.86	23.04
CdTe/ZnO	0.888	33.82	76.92	23.13
CdTe/ZnS	0.877	34.46	81	24.48

4.2. Analysis with alternative structures

Two alternative solar cell configurations were explored: NiO/CdTe/IGZO/ITO and NiO/CdTe/CdS/IGZO/ITO. These structures aim to enhance the efficiency of CdTe-based solar cells by incorporating materials that improve charge transport and minimize energy losses. In the first configuration (NiO/CdTe/IGZO/ITO), NiO serves as the hole transport layer (HTL), while IGZO functions as a buffer layer. The second configuration (NiO/CdTe/CdS/IGZO/ITO) introduces an additional CdS layer, where NiO continues to act as the HTL, IGZO functions as the electron transport layer (ETL), and CdS is positioned between the CdTe and IGZO layers to serve as a buffer.

For the simulations, the layer thicknesses were set as follows: NiO (0.03 μm), CdTe (5 μm), IGZO (0.03 μm), CdS (0.03 μm), and ITO (0.5 μm). These parameters were used to analyze the relationship between open-circuit voltage (Voc) and short-circuit current density (Jsc), providing insights into the efficiency of each configuration. The NiO/CdTe/IGZO/ITO structure demonstrated improved performance due to the inclusion of NiO, which has a wide bandgap and high hole mobility. NiO effectively aligns with the CdTe valence band, facilitating efficient hole transport while minimizing recombination losses. This results in an increase in Voc and fill factor (FF), ultimately enhancing power conversion efficiency (PCE).

The NiO/CdTe/CdS/IGZO/ITO configuration further optimizes performance by introducing the CdS buffer layer. The presence of CdS helps to smooth out the interface between CdTe and IGZO, reducing defects that can contribute to recombination losses. Additionally, the wider bandgap of CdS creates a graded bandgap structure, improving charge separation and collection. This results in a higher Voc of 1.1735 V, an FF of 86.96%, and an impressive PCE of 29.59%. The improved alignment between CdS and CdTe further enhances device performance, leading to more efficient carrier transport and overall stability.

A comparative analysis of both configurations highlights that the NiO/CdTe/CdS/IGZO/ITO structure offers superior performance due to its enhanced interface quality and charge transport dynamics. The simulation results, along with comparisons to existing structures, are summarized in Table 4. The corresponding Jsc-Voc graph in Figure 3(b) clearly illustrates the superior efficiency of the NiO/CdTe/CdS/IGZO/ITO configuration.

Table 4. Comparison with different existing structure with CdTe as the active layer and NiO as HTL.

Solae cell Structure	Voc(V)	Jsc(mA/cm^2)	FF(%)	Eta(%)
NiO/CdTe/IGZO/ITO	1.1178	30.099	83.26	28.01
NiO/CdTe/CdS/IGZO/ITO	1.1735	28.996	86.96	29.59
NiO/CdTe/CdS/FTO	1.09	27.38	87.85	26.35
NiO/CdTe/CdS/ZnO	1.06	24.56	86.46	22.42

5. Conclusion

This study evaluated the dual role of IGZO as both a buffer layer and an electron transport layer (ETL) in CdTe-based solar cells using SCAPS 1D simulations. CdTe was employed as the primary absorber layer, and its performance was analyzed with four different transparent conducting oxides (TCOs): SnO_2, ZnO, ITO, and FTO. Among these, the CdTe/IGZO/ITO configuration demonstrated superior efficiency, achieving Voc = 1.0414 V, Jsc = 26.99 mA/cm², FF = 87.11%, and η = 24.48%, marking a significant improvement over other structures. To further enhance performance, two new configurations were introduced: NiO/CdTe/IGZO/ITO and NiO/CdTe/CdS/IGZO/ITO. In the first structure, NiO served as the hole transport layer (HTL), while IGZO functioned as a buffer layer. The second configuration incorporated a CdS buffer layer between CdTe and IGZO, enabling IGZO to act as an ETL. This modification significantly improved efficiency, with the NiO/CdTe/CdS/IGZO/ITO structure achieving Voc = 1.1735 V, Jsc = 28.996 mA/cm², FF = 86.96%, and η = 29.59%, outperforming both the NiO/CdTe/IGZO/ITO structure and previously reported designs such as NiO/CdTe/CdS/FTO and NiO/CdTe/CdS/ZnO.

A comprehensive analysis of the NiO/CdTe/CdS/IGZO/ITO solar cell examined the impact of key parameters, including layer thickness, carrier densities, defect densities, shunt resistance (Rsh), and series resistance (Rs). The optimized values were determined as follows:

1. Acceptor densities: NiO (10^{21} cm^{-3}), CdTe (10^{17} cm^{-3})
2. Donor densities: CdS (10^{16} cm^{-3}), IGZO (10^{17} cm^{-3}), ITO (10^{17} cm^{-3})
3. Resistances: Rsh = 5.8 kΩ, Rs = 5.26 Ω
4. CdTe defect density: 10^{13} cm^{-3}
5. Optimized layer thicknesses: NiO (0.03 μm), CdTe (5 μm), CdS (0.03 μm), IGZO (0.03 μm), and ITO (0.5 μm)

Using these optimized parameters, simulations confirmed the superior performance of the NiO/CdTe/CdS/IGZO/ITO structure, reaffirming its potential for high-efficiency applications.

Future research can build on these findings by exploring advanced doping strategies for IGZO and CdS to further reduce recombination losses and enhance charge carrier mobility. Additionally, integrating CdTe with emerging materials such as perovskites in tandem solar cell configurations may unlock even higher efficiencies. Experimental validation of these simulations will be crucial in addressing real-world challenges, including device stability, cost-effectiveness, and scalability, ensuring that these advancements translate into practical solar cell technologies.

References

[1] Q. Hassan, P. Viktor, T. J. Al-Musawi, B. M. Ali, S. Algburi, H. M. Alzoubi, A. K. Al-Jiboory, A. Z. Sameen, H. M. Salman, M. Jaszczur, Renewable Energy Focus **48**, 100545 (2024).https://doi.org/10.1016/j.ref.2024.100545

[2] S. Sivaraj, R. Rathanasamy, G.V. Kaliyannan, H. Panchal, A.J. Alrubaie, M.M. Jaber, Z. Said, S. Memon, Energies **15**(22), 8688 (2022).https://doi.org/10.3390/en15228688

[3] W. Shockley, H. J. Queisser, Journal of Applied Physics **32**(3), 510 (1961). https://doi.org/10.1063/1.1736034

[4] M. A. Green, E. D. Dunlop, J. Hohl-Ebinger, Progress in Photovoltaics: Research and Applications 31(1), 1 (2023). https://doi.org/10.1002/pip.3726

[5] N. L. Muttumthala, A. Yadav, Materials Today: Proceedings 64, 1475 (2022).https://doi.org/10.1016/j.matpr.2022.04.862

[6] A. Bosio, D. Menossi, S. Mazzamuto, N. Romeo, Thin Solid Films 519(21), 7522 (2011).https://doi.org/10.1016/j.tsf.2010.12.137

[7] G. Agostinelli, P.-J. Alet, A. Bett, F. Bonemazzi, P. Boydell, B. Dimmler, D. Dimova-Malinovska, P. Fath, F. Ferrazza, A. Galdikas, S. Glunz, S. Krawietz, P. Malbranche, O. Mayer, P. Mints, N. Pearsall, J. Poortmans, M. Powalla, C. Protogeropoulos, P. Vanbuggenhout, "A Strategic Research Agenda for Photovoltaic Solar Energy Technology", 2011.https://doi.org/10.2788/15824

[8] A. Morales-Acevedo, Solar Energy 80(6), 675 (2006).https://doi.org/10.1016/j.solener.2005.10.008

[9] A. Romeo, E. Artegiani, Energies 14(6), 1684 (2021).https://doi.org/10.3390/en14061684

[10] J. N. Sameera, M. A. Islam, S. Islam, T. Hossain, M. K. Sobayel, M. Akhtaruzzaman, N. Amin, M. J. Rashid, Optical Materials 123, 111911 (2022).https://doi.org/10.1016/j.optmat.2021.111911

[11] L. Hafaifa, M. Maache, Z. Allam, A. Zebeir, Results in Optics 14, 100596 (2024).https://doi.org/10.1016/j.rio.2023.100596

[12] D.-B. Li, Z. Song, R. A. Awni, S. S. Bista, N. Shrestha, C. R. Grice, L. Chen, G. K. Liyanage, M. A. Razooqi, A. B. Phillips, M. J. Heben, ACS Applied Energy Materials 2(4), 2896 (2019).https://doi.org/10.1021/acsaem.9b00233

[13] J. C. Z. Medina, E. R. Andrés, C. M. Ruíz, E. C. Espinosa, L. T. Yarce, R. Galeazzi Isasmendi, R. R. Trujillo, G. G. Salgado, A. C. Solis, F. G. N. Caballero, Coatings 13, 1436 (2023). https://doi.org/10.3390/coatings13081436.

[14] P. Zhan, J. Chen, L. Chen, IOP Conference Series: Earth and Environmental Science 781, 042069 (2021). https://doi.org/10.1088/1755-1315/781/4/042069

[15] G. T. Chavan, Y. Kim, M. Q. Khokhar, S. Q. Hussain, E.-C. Cho, J. Yi, Z. Ahmad, P. Rosaiah, C.-W. Jeon, Nanomaterials 13, 1226 (2023). https://doi.org/10.3390/nano13071226

[16] C. Hwang, T. Kim, Y. Jang, D. Lee, H.-D. Kim, Nanomaterials 14(22), 1841 (2024). https://doi.org/10.3390/nano14221841

[17] M. Burgelman, P. Nollet, S. Degrave, Thin Solid Films **361–362**, 527 (2000).

[18] M. K. Hossain, A. A. Aktab, R. C. Das, K. Hossain, M. H. K. Rubel, Md. Rahman, H. Bencherif, M. Emetere, K. Mustafa, R. Pandey, RSC Advances 12, 35002 (2022). http://doi.org10.1039/d2ra06734j.

[19] L. I. Nykyruy, V. P. Petrova, S. M. Ivanov, Optical Materials 92, 319 (2019).https://doi.org/10.1016/j.optmat.2019.04.029